Chapter 2
Radiation-Matter Interactions

The behavior of radiation and matter as a function of energy governs the degradation of astrophysical information along the path and the characteristics of the detectors. This chapter firstly presents the mechanisms of the energy loss of charged particles in matter: ionization, bremsstrahlung, Cherenkov radiation, transition radiation, nuclear reactions; in addition, the effect of multiple scattering will be summarized. Then the chapter discusses the mechanisms of photon interactions: photoelectric effect, Compton effect, pair production. The characteristic scales of electromagnetic (radiation length) and nuclear (interaction length) processes are discussed. The discussed effects are the foundation for the detectors discussed in the following. The nature of fundamental fluctuations related to the detection processes will be outlined. The interactions of radiation and particles are presented without formally deriving the relative cross sections, but rather elaborating on the critical factors leading to the detector construction.

2.1 Interactions of Charged Particles

Charged particles interact mostly with electrons and loose energy through different mechanisms [1–7]:

- Ionization and excitation of atoms encountered along the path
- Bremsstrahlung
- Cherenkov Radiation
- Transition Radiation

In addition, charged particles undergo multiple scattering that produces a series of small deviations from the path that increases its effective length.

R. Poggiani, *High Energy Astrophysical Techniques*,
UNITEXT for Physics, DOI 10.1007/978-3-319-44729-2_2

2.1.1 Energy Loss by Ionization

A charged particle in matter looses energy by *ionization* and *excitation* of the atoms along the path, transferring energy to the atomic electrons. The key parameter is the maximum amount of energy transferred in a single collision. The energy loss is different for heavy particles and electrons/positrons, due to their mass, that must be compared with the mass of target electrons. The energy loss per unit length of heavy charged particles, or *stopping power*, is described by the Bethe-Bloch equation [2]:

$$-\frac{dE}{dx} = 4\pi N_A r_e^2 m_e c^2 \frac{Z}{A}\frac{z^2}{\beta^2}\left[\ln\frac{2m_e c^2\beta^2\gamma^2}{I} - \beta^2 - \frac{\delta}{2}\right] \tag{2.1}$$

where N_A is the Avogadro number, r_e is the classical electron radius, m_e is the electron mass, z is the charge number of the incident particle, Z, A are the atomic mass and number of the medium, I the mean excitation energy of the medium, δ the density effect correction. The mean excitation energy can be approximated by $I = 16 \cdot Z^{0.9}$ eV. Since $\frac{Z}{A}$ is close to $\frac{1}{2}$ for most media, the ionization energy loss shows a weak dependence on the material and the stopping power can be approximated by the product of the square of the particle charge and of a function of its velocity:

$$-\frac{dE}{dx} = z^2 f(\beta) \tag{2.2}$$

The behavior of the stopping power for protons in silicon is shown in Fig. 2.1.

The Bethe-Bloch equation (Eq. 2.1) shows an energy loss proportional to $1/\beta^2$ at low energies and a logarithmic rise at high energies. The density correction takes into account the effect of the polarization of the medium that produces a screening of the electric field of the incident particle: the ionization loss approaches a plateau at high energies.

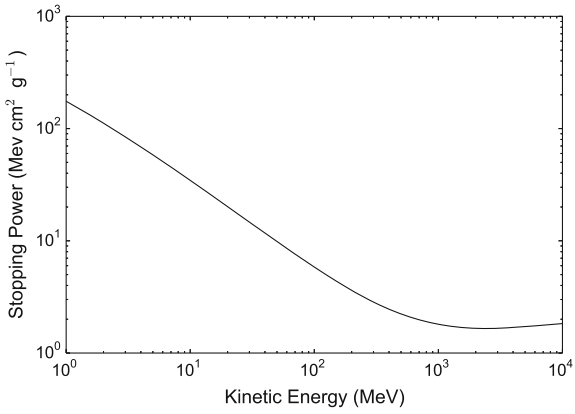

Fig. 2.1 Energy loss by ionization for protons in silicon, based on the data available at http://www.nist.gov/pml/data/star/

The ionization loss shows a minimum at $\beta\gamma \sim 4$. The energy loss of a *minimum ionizing particles*, called *mip*, is:

$$-\left(\frac{dE}{dx}\right)_{minimum} \sim 2\ MeV\ g^{-1}\ cm^2 \tag{2.3}$$

For example, the energy loss of a *mip* crossing 1 cm of a plastic scintillator, that has a density of about 1 g cm^{-2}, is about 2 MeV. Cosmic ray muons and relativistic particles in general are examples of the *minimum ionizing particles*. The energy loss of different particles is different in the region below the minimum of ionization and can be used to identify the type particles. The ionization loss for protons, electron and helium ions in air is shown in Fig. 2.2.

Very rarely, the energy transfer from the projectile to the electrons is large enough to allow them to produce additional ionization; the knock-on electrons are called δ-rays.

During the interaction of the charged particle with the medium, there will be fluctuations in the energy loss, whose properties depend on the thickness of the absorber material. The Bethe-Bloch equation (Eq. 2.1) describes only the average energy loss of particles. The distribution of the energy loss is a Gaussian with thick absorbers, due to the large number of collisions, but becomes asymmetrical in thin absorbers, where it is described by the *Landau distribution* [2, 6]:

$$Ł_\lambda = \frac{1}{2\pi} \exp\left[-\frac{1}{2}(\lambda + e^{-\lambda})\right] \tag{2.4}$$

where the parameter λ is given by:

$$\lambda = \frac{\Delta E - \Delta_{mp}}{\xi} \tag{2.5}$$

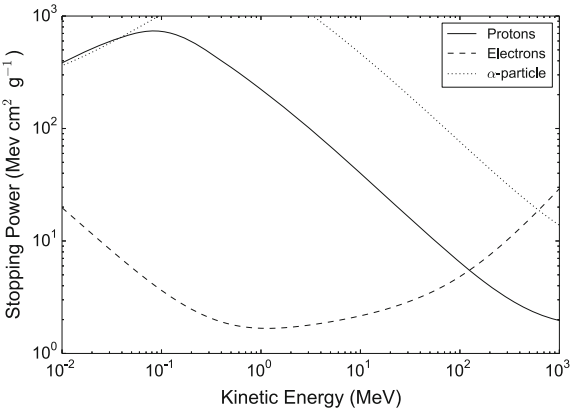

Fig. 2.2 Energy loss of protons, electrons and helium ions in air, based on the data available at http://physics.nist.gov/PhysRefData/Star/Text/intro.html

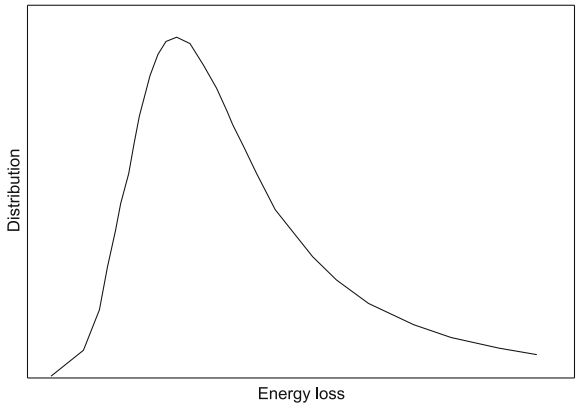

Fig. 2.3 Landau energy loss

and describes the deviation of the energy loss from the most probable energy loss [2, 6]:

$$\Delta_{mp} = \xi \left[\ln \frac{2m_e c^2 \beta^2 \gamma^2}{I} + \ln \frac{\xi}{I} + 0.200 - \beta^2 - \delta \right] \tag{2.6}$$

where $\xi = 2\pi N_A r_e^2 m_e c^2 \frac{Z}{A} z^2 \frac{d}{\beta^2}$, d is the absorber thickness in units of g cm^{-2}. The Landau distribution has a tail on the side of high energies (Fig. 2.3).

The ionization energy loss of electrons is different from the ionization of heavy particles since the projectile and the target share the same mass and differs also from the energy loss of positrons. The maximum energy transfer from incident electrons to atomic electrons is half the kinetic energy. The stopping power for electron-electron and electron-positron scattering is given by [2]:

$$-\frac{dE}{dx} = 4\pi N_A r_e^2 m_e c^2 \frac{Z}{A} \frac{1}{\beta^2} \left[\ln \frac{m_e c^2 \beta \gamma \sqrt{\gamma - 1}}{\sqrt{2} I} + F^* \right] \tag{2.7}$$

where F^* is a different function depending on the incident particle, electron or positron [2]. We will see later that the total energy loss of electrons must include the bremsstrahlung, a radiative process.

The energy loss is the key stone of several families of detectors that will be described in the next chapters. In addition to loosing energy by ionization, a charged particle traversing a medium undergoes multiple scattering events due to the Coulomb interaction with nuclei, according to the Rutherford scattering law. During its path, the charge will experience a large number of scatterings with small deviations from the original trajectory. The *multiple Coulomb scattering* is described by the Moliere theory. Assuming that the scattering angles are small, the distribution of the scattering angles will be a Gaussian. The rms width of the projected distribution of the scattering angles is [2]:

$$\theta_{scattering} = \frac{13.6MeV}{\beta cp} z \sqrt{\frac{d}{X_0}} \left[1 + 0.038 \ln \frac{d}{X_0} \right] \tag{2.8}$$

where d is the medium thickness, p is the momentum of the particle in MeV/c, z its charge, X_0 is the radiation length that will be discussed in detail in the next section.

2.1.2 Bremsstrahlung

A charged particle in a medium will loose energy not only by ionization, by also by interaction with the Coulomb field of the nuclei of the material. When decelerated in the nuclear field, the particle will loose energy by emitting photons in the *bremsstrahlung* process. The energy loss by bremsstrahlung for a charge with mass m, charge number z and energy E is [2]:

$$-\frac{dE}{dx} = 4\alpha N_A \frac{Z^2}{A} z^2 \left(\frac{1}{4\pi\epsilon_0} \frac{e^2}{mc^2} \right)^2 E \ln \frac{183}{Z^{\frac{1}{3}}} \tag{2.9}$$

where Z, A are the atomic number and mass of the medium. The dependence on the reciprocal of the squared mass of the projectile suggests that bremsstrahlung is more relevant for light particles, such as electrons. The photons are emitted within a typical angle of the order of $\sim \frac{m_e c^2}{E}$. The energy loss by bremsstrahlung is proportional to the particle energy, while the energy loss by ionization is proportional to the logarithm of energy: the bremsstrahlung will be the dominant source of losses at high energies (Fig. 2.4).

The radiation loss by bremsstrahlung is characterized by the *radiation length* X_0, the mean distance required to reduce the particle energy to a fraction $1/e$ of the initial value:

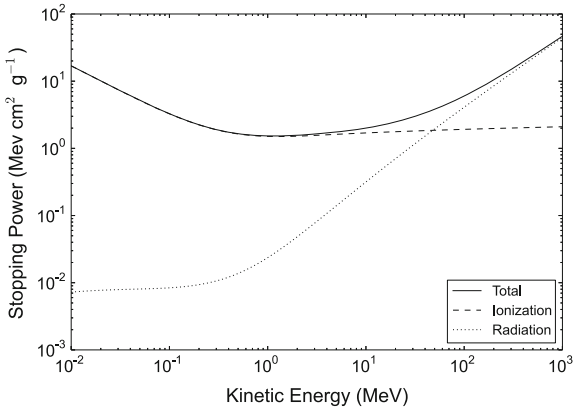

Fig. 2.4 Ionization energy loss and bremsstrahlung loss for electrons in silicon; data from http://physics.nist.gov/PhysRefData/Star/Text/ESTAR.html

Table 2.1 Radiation length, critical energy, Moliere radius (Chap. 3), interaction length, density for materials of interest in detection (*Source* http://pdg.lbl.gov/2015/AtomicNuclearProperties/)

Material	X_0 (g cm^{-2})	E_c (MeV)	R_M (g cm^{-2})	λ_I (g cm^{-2})	ρ (g cm^{-3})
Air (1 atm)	36.62	87.92	8.83	90.1	$1.20 \cdot 10^{-3}$
Water	36.08	78.33	9.77	83.3	1.00
NaI	9.49	13.37	15.05	154.6	3.67
Polystyrene	43.79	93.11	9.97	81.7	1.06
Si	21.82	40.19	11.51	108.4	2.33
Pb	6.37	7.43	18.18	199.6	11.4
Emulsion	11.33	17.43	13.79	135.1	3.82
Liquid argon	19.55	32.84	12.62	119.7	1.40

$$-\left(\frac{dE}{dx}\right)_{radiative} = \frac{E}{X_0} \tag{2.10}$$

The radiation length X_0 depends on the material properties, the atomic number and mass:

$$X_0 = \frac{A}{4\alpha N_A Z(Z+1) r_e^2 \ln(183 Z^{-\frac{1}{3}})} \tag{2.11}$$

Some typical values of the radiation length are reported in Table 2.1.

The *critical energy* is the energy where the loss rates by ionization and by bremsstrahlung are equal. An approximation of the critical energy in solids is [2]:

$$E_c \sim \frac{610}{Z + 1.24} MeV \tag{2.12}$$

The critical energy is of the order of tens MeV in common materials (Table 2.1).

The complicate path of a charged particle in an absorber has triggered the construction if empirical *range-energy relations*, fundamental for the building detectors. The *range* of a particle is formally defined as:

$$R = \int_E^0 \frac{dE}{\frac{dE}{dx}} \tag{2.13}$$

However, the effective dependence of the energy loss on energy is very complex and charged particles undergo multiple scattering. The range is better defined for heavier particles, since they are less affected by scattering. Several works have addressed the specific ranges of particles in selected materials and for different interval of energies. Generally, range-energy relations can be summarized by a power law in energy. An example of interest for astroparticle physics is the range of muons in rock in Fig. 2.5.

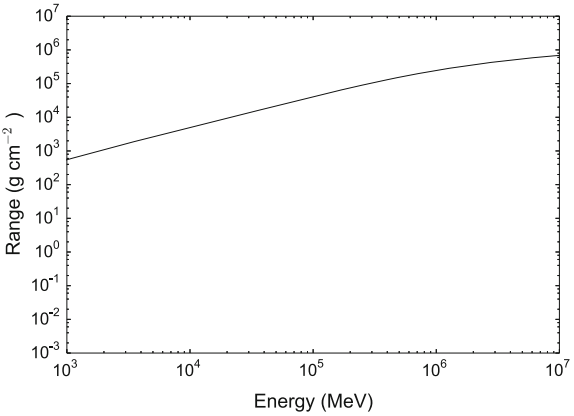

Fig. 2.5 Range of muons in rock as a function of energy; data from http://pdg.lbl.gov/2015/AtomicNuclearProperties/

2.1.3 Cherenkov Radiation

The Cherenkov radiation is emitted when a charged particle travels in a medium at a speed larger than the light speed in the medium. The velocity of light in a medium with index of refraction n is $\frac{c}{n}$. The Cherenkov effect is similar to the mechanism of the supersonic boom of a plane. The electric field of the traveling charge polarizes the medium that reverts to the previous unpolarized state afterwards, producing an electromagnetic perturbation. The combination of the perturbations events builds a single wavefront traveling along the charged particle direction at the speed of light in the medium. The angle θ_c that defines the direction of photon emission is:

$$\cos\theta_c = \frac{1}{n\beta} \tag{2.14}$$

where $\beta = \frac{v}{c}$ is the particle speed. The intensity of Cherenkov radiation per energy interval and path length interval is [3, 6]:

$$\frac{d^2N}{dEdx} = \frac{z^2\alpha}{\hbar c}\left(1 - \frac{1}{n^2\beta^2}\right) \tag{2.15}$$

where z is the particle charge. The photon yield per unit wavelength is:

$$\frac{dN}{d\lambda} = \frac{2\pi z^2\alpha}{\lambda^2}\left(1 - \frac{1}{n^2\beta^2}\right) \tag{2.16}$$

The yield of visible light is about $500\, z^2 \sin^2\theta_c$ photons per cm. The spectrum has a peak in the high frequency region, thus the Cherenkov radiation appears as blue light. The properties of some materials used in Cherenkov detectors is presented in Table 2.2.

Table 2.2 Index of refraction and Cherenkov threshold of some materials [2]

Material	n − 1	Threshold β
Air (STP)	$2.9 \cdot 10^{-4}$	0.9997
Water	0.333	0.7501
Ice	0.309	0.7639
Polystyrene	0.59	0.6289

The Cherenkov effect is used to measure the properties of the charged particles emitted in the electromagnetic and hadronic showers (Chap. 3) induced by high energy gamma rays and cosmic rays in the atmosphere. For reference, the Cherenkov threshold of electrons in air at Standard Temperature and Pressure (STP) is 21 MeV, while the emission angle of the radiation is about 1.3° at the Standard Temperature and Pressure. The Cherenkov effect is used also to detect the charged products of the interactions of neutrinos with matter (Chap. 14).

The energy loss by Cherenkov radiation is much smaller than the loss by ionization. However, its detection is the signature that the incident particle velocity is above the threshold. The combination of the velocity with the energy information estimated by other methods provides the mass of the particle and its identification.

2.1.4 Transition Radiation

The Transition Radiation is an effect related to the polarization of the medium produced by the passage of a charged particle. When a charge in relativistic motion crosses the boundary between two media with different dielectric properties, photon emission occurs. The effect depends on the plasma frequency ω_p of the medium [2]:

$$\hbar\omega_p = \frac{m_e c^2}{\alpha}\sqrt{4\pi n_e r_e^3} \tag{2.17}$$

where n_e is the electron number density. For most materials the plasma energy is of the order of some tens eV. The spectrum of the emitted photons shows a steep decrease for energies larger than $\gamma\hbar\omega_p$. An estimation of the magnitude of the photon energy is about $\frac{\gamma\hbar\omega_p}{4}$. The total energy emitted when the charge crosses the boundary between the vacuum and a medium is [2]:

$$E = \frac{1}{3}\alpha z^2 \gamma \hbar\omega_p \tag{2.18}$$

The most part of the radiation is emitted within a cone with a semi-aperture angle of about $\frac{1}{\gamma}$. The amount of emitted energy is proportional to the relativistic factor, thus the Transition Radiation can be used for the identification of the particle type. For very fast particles, with γ of the order of thousands, the

emitted photons are in the soft X-rays region of the spectrum. The number of photons emitted above a threshold $E_{th} = \hbar\omega_0$ is:

$$N_{trd} = \alpha \frac{z^2}{\pi} \left[\left(\ln \frac{\gamma \hbar \omega_p}{\hbar \omega_0} - 1 \right)^2 + \frac{\pi^2}{12} \right] \tag{2.19}$$

2.2 Interactions of Photons

Photons are detected by the production of charged particles in their interactions with matter. The interactions of photons occur through three main processes: the *photoelectric effect*, *Compton scattering* and *pair production*. Typically, the interaction produces electrons that are later measured by their ionization loss.

2.2.1 Photoelectric Effect

The photoelectric effect is described by the process [2, 5, 6]:

$$\gamma + atom \rightarrow atom^* + e^- \tag{2.20}$$

The atomic electrons absorb the energy of an incident photon, a process forbidden to free electrons by the momentum conservation; the process is assisted by a third body, the atomic nucleus, that deals with the recoil momentum. The cross section of photoelectric effect shows some peculiar edges superposed to a smoothly curve decreasing with energy. The edges correspond to the absorption of photons to a specific shell; the K shell gives the dominant contribution. In the regions far from the absorption edges the total photoelectric cross section is given by:

$$\sigma_{photoelectric} = \sqrt{\frac{32}{(\frac{E}{m_e c^2})^7}} \alpha^4 Z^5 \sigma_{Thomson} \tag{2.21}$$

where E is the photon energy and $\sigma_{Thomson} = \frac{8}{3}\pi r_e^2$ is the *Thomson cross section* describing the elastic scattering of photons on electrons. The photoelectric effect is particularly important for X-ray detectors. When photoelectric effect involves an inner atomic shell, two additional effects can occur. If the empty place is filled by an electron coming from an higher shell, there will be emission of X-rays. The energy budget, if larger than the typical energy of a shell, can produce the ejection of a second electron, in the Auger effect.

2.2.2 Compton Scattering

The Compton effect is the scattering of photons on atomic electrons, that can be assumed to be almost free [2, 5, 6]:

$$\gamma + e^- \rightarrow \gamma + e^- \tag{2.22}$$

The total cross section for the Compton scattering per electron is described by the Klein-Nishina formula:

$$\sigma^e_{Compton} = 2\pi r_e^2 \left[\left(\frac{1+\varepsilon}{\varepsilon^2} \right) \left(\frac{2(1+\varepsilon)}{1+2\varepsilon} - \frac{1}{\varepsilon} \ln(1+2\varepsilon) \right) + \frac{1}{2\varepsilon} \ln(1+2\varepsilon) - \frac{1+3\varepsilon}{(1+2\varepsilon)^2} \right] \tag{2.23}$$

where $\varepsilon = \frac{E}{m_e c^2}$, E is the initial energy of the photon. For an atom with Z electrons, the scattering cross section will be $Z\sigma^e_{Compton}$. While the photoelectric effect is a pure absorption of the energy of a photon, Compton effect involves only a partial transfer of energy to the electron. The total Compton cross section can be split between the scattering cross section and the absorption cross section:

$$\sigma^{scattering}_{Compton} = \frac{E_f}{E} \sigma^e_{Compton} \tag{2.24}$$

$$\sigma^{absorption}_{Compton} = \sigma^e_{Compton} - \sigma^{scattering}_{Compton} \tag{2.25}$$

where E_f is the final energy of the photon. The relevant quantities from the point of view of detection are the differential distributions of the scattered electrons, in solid angle and in energy:

$$\frac{d\sigma^e_{Compton}}{d\Omega} = \frac{r_e^2}{2} \left(\frac{E_f}{E} \right)^2 \left[\frac{E}{E_f} - \frac{E_f}{E} - \sin^2\theta \right] \tag{2.26}$$

$$\frac{d\sigma^e_{Compton}}{dT_e} = \frac{d\sigma^e_{Compton}}{d\Omega} \frac{2\pi}{\varepsilon^2 m_e c^2} \left[\frac{(1+\varepsilon)^2 - \varepsilon^2 \cos^2\theta_e}{(1+\varepsilon)^2 - \varepsilon(2+\varepsilon)\cos^2\theta_e} \right]^2 \tag{2.27}$$

where E, E_f are the energies of incident and scattered photons, θ, θ_e are the scattering angles of photon and electron, T_e the kinetic energy of electron. The energy distribution of the Compton recoil electrons is shown in Fig. 2.6.

The distribution has a cut-off, the *Compton edge*. The Compton effect is used to build detection systems for γ-rays in the regions of tens MeV. The *inverse Compton scattering*, where high energy electrons scatter on low energy photons and increase their frequency is very common in high energy astrophysics.

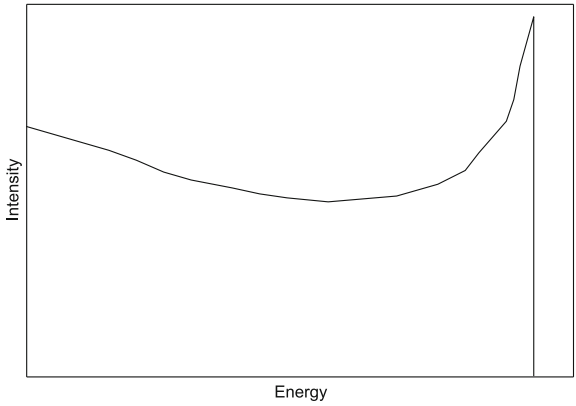

Fig. 2.6 Compton effect: energy distribution of the recoil electron

2.2.3 Pair Production

Pair production occurs when a photon converts to an electron-positron pair in the Coulomb field of a nucleus [2]:

$$\gamma + nucleus \rightarrow e^- + e^+ + nucleus \tag{2.28}$$

The process has a threshold given by the sum of the rest masses of electrons and positrons and the recoil energy of the nucleus:

$$E_{threshold} = 2m_e c^2 + 2\frac{m_e^2 c^2}{m_{nucleus}} \sim 2m_e c^2 \tag{2.29}$$

Due to the large nuclei masses, the threshold can be approximated by twice the electron mass, $2m_e c^2$.

The pair production cross section depends on the degree of screening of the nuclear charge by the atomic electrons, that depends on the photon energy. The condition of no screening or complete screening depends on the value of ε, the photon energy normalized to the electron rest mass, with respect to the quantity $\frac{1}{\alpha Z^{\frac{1}{3}}}$. The pair production cross sections for no screening and complete screening are given by:

$$\sigma_{pair}^{ns} = 4\alpha r_e^2 Z^2 \left(\frac{7}{9}\ln 2\varepsilon - \frac{109}{54}\right) \tag{2.30}$$

$$\sigma_{pair}^{cs} = 4\alpha r_e^2 Z^2 \left(\frac{7}{9}\ln \frac{183}{Z^{\frac{1}{3}}} - \frac{1}{54}\right) \tag{2.31}$$

The complete screening cross section corresponds to energetic photons and does not depend on their initial energy. Dropping the last term inside the brackets of the complete screening equation, the cross section becomes:

$$\sigma_{pair}^{cs} \sim 4\alpha r_e^2 Z^2 \left(\frac{7}{9}\ln\frac{183}{Z^{\frac{1}{3}}}\right) \sim \frac{7}{9}\frac{A}{N_A}\frac{1}{X_0} \tag{2.32}$$

The length scale λ_{pair} of the pair production is related to the radiation length X_0 by the relation:

$$\lambda_{pair} = \frac{9}{7}X_0 \tag{2.33}$$

i. e. by a factor $\frac{7}{9}$. The close values of the typical lengths of the two processes will be relevant in the production of a cascade of particles started by a high energy photon or electron, that will be discussed in Chap. 3.

2.2.4 Total Cross Section for Photons

In view of designing detectors, it is useful to introduce the concept of *absorption coefficient* μ, that governs the attenuation of a photon beam in matter:

$$I = I_0 e^{-\mu x} \tag{2.34}$$

The absorption coefficient summarizes the role of the cross sections σ_i of the different interaction mechanisms σ_i:

$$\mu = \frac{N_A}{A}\sum_i \sigma_i \tag{2.35}$$

The absorption coefficient inherits the energy dependence of the physical processes mentioned above. The contribution of the photoelectric effect, Compton effect and pair production to the absorption coefficients of photons in silicon is shown in Fig. 2.7.

The photoelectric effect dominates at low energies (below some hundreds keV), the Compton scattering in the intermediate (MeV) region, while pair production is the most relevant mechanism at high energy (above some MeV). The energy dependence has a strong impact on the building of instrumentation for X-ray and gamma-ray astrophysics, as it will be discussed in Chaps. 11, 12.

In view of designing detectors for high energy photons, we briefly recall the dependence of the cross sections on the atomic number Z of the absorber material. The photoelectric effect depends on Z^5, the Compton effect on Z, the pair production on Z^2: thus detectors for high energy photons should be built with high Z materials.

For reference, we report the absorption coefficient of photons in two common detector materials, the heavy scintillator CsI and a plastic scintillator, in Fig. 2.8.

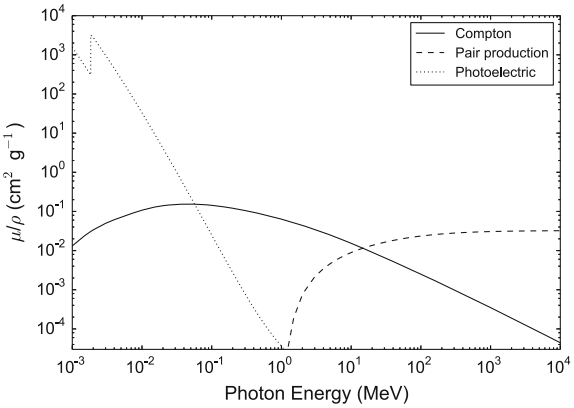

Fig. 2.7 Contribution of the photoelectric effect, the Compton effect and the pair production to the absorption coefficient of photons in silicon (data from NIST)

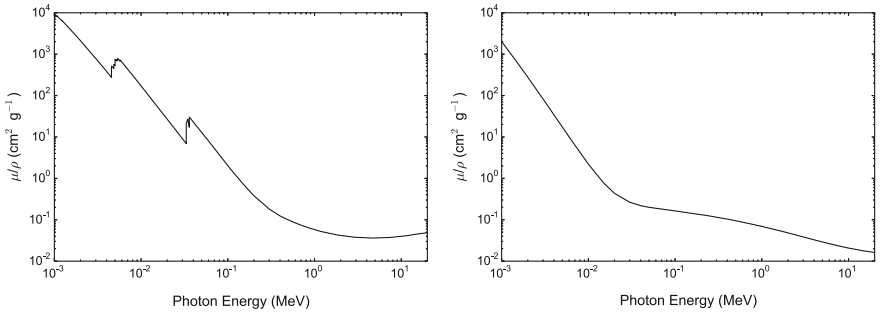

Fig. 2.8 Photon absorption coefficient for the heavy scintillator CsI (*left*) and for plastic scintillator (*right*); data from http://physics.nist.gov/PhysRefData/XrayMassCoef/tab4.html

2.3 Interaction of Hadrons

Hadrons interact with matter through strong interactions, in addition to the electromagnetic ones [2]. The majority of process belonging to this class involve inelastic scattering events that produce additional hadronic particles. The details of the interaction depend on the nature of the incident particle, a proton or a nucleus, and on its energy. The geometrical cross section for the proton-proton interaction is of the order of the squared proton radius, $\sim 10^{-26}$ cm^2; since a nucleus with atomic mass A has a size $A^{\frac{1}{3}}$, the corresponding cross section will be $A^{\frac{2}{3}}$ times larger than the proton cross section.

From the practical point of view, the large variety of strong processes accounted for by the cross section σ_h is summarized by the *hadronic interaction length* λ_{int}:

$$\lambda_{int} = \frac{A}{N_A \rho \sigma_{inelastic}} \tag{2.36}$$

where $\sigma_{inelastic}$ is the inelastic part of the cross section. The interaction length of some materials is reported in Table 2.1. The interaction length plays, for hadron reactions, the same role of the radiation length for electromagnetic interactions. An high energy hadron, a proton or a nucleus, will experience a nuclear interaction after one interaction length, while loosing only a small energy by ionization. The collision will produce additional hadrons and will break the target nucleus into several nuclear fragments. A large part of the secondary particles are charged or neutral pions. The secondary hadrons can trigger further particle production, leading to a cascade.

Problems

2.1 Discuss the mechanisms of energy loss for charged particles and their behavior as a function of energy.

2.2 Discuss the mechanisms of interaction of photons with matter and their behavior as a function of energy.

References

1. De Angelis, A., Pimenta, M.J.M.: Introduction to Particle and Astroparticle Physics. Springer-Verlag Italia, (2015)
2. Grupen, C. and Swartz, B.: Particle Detectors. Cambridge University Press (2008)
3. Grupen, C. and Buvat, I: Handbook of Particle Detection and Imaging. Springer-Verlag Berlin Heidelberg (2012)
4. Lèna, P. et al.: Observational Astrophysics. Springer-Verlag Berlin Heidelberg (2012)
5. Leo, W. R.: Techniques for Nuclear and Particle Physics Experiments - A How-to Approach. Springer-Verlag (1994)
6. Olive, K.A. et al. (Particle Data Group): Chin. Phys. C **38**, 090001 (2014)
7. Spurio, M.: Particles and Astrophysics - A Multi-Messenger Approach. Springer International Publishing, Switzerland (2015)

http://www.springer.com/978-3-319-44728-5

High Energy Astrophysical Techniques
Poggiani, R.
2017, XIV, 163 p. 64 illus., Hardcover
ISBN: 978-3-319-44728-5